

In Situ Synchrotron Radiation Powder X-ray Diffraction

study of the $2\text{LiNH}_2 + \text{LiH} + \text{KBH}_4$ system

Maddalena Sale¹, Claudio Pistidda², Alessandro Taras¹, Emilio Napolitano¹, Chiara Milanese³, Fahim Karimi², Martin Dornheim², Sebastiano Garroni^{1*}, Stefano Enzo¹ and Gabriele Mulas¹

¹Department of Chemistry and Pharmacy, University di Sassari and INSTM, Via Vienna 2, I-07100 Sassari, Italy

²Institute of Materials Research, Materials Technology, Helmholtz-Zentrum Geesthacht, Max-Planck, Str. 1, D-21502 Geesthacht, Germany

³Pavia H₂ Lab, C.S.G.I. & Dipartimento di Chimica, Sezione di Chimica Fisica, Università di Pavia, Viale Taramelli 16, I-27100 Pavia, Italy

* Corresponding author: Sebastiano Garroni

Phone: +39 079 229524

Fax: +39 079 229559

E-mail address: sgarroni@uniss.it

ABSTRACT:

In the present work we focus on the $2\text{LiNH}_2 + \text{KBH}_4 + \text{LiH}$ system: the phase-structural transformations occurring during the desorption process on the powder mixture are described by in-situ Synchrotron Radiation Powder X-ray Diffraction (SR-PXD), high-pressure differential scanning calorimetry and manometric measurements. It is observed that LiNH_2 transforms into Li_2NH during heating, at about 160°C , while the reflections related to KBH_4 disappeared at 380°C . At higher temperature, the formation of Li_3BN_2 is detected, together with an evident increase of the background, ascribable to the presence of a further phase in the molten state. Patterns at room temperature, after cooling down the sample, confirm the presence of Li_3BN_2 and KH as reported in the theoretical study. For the as prepared mixture it is possible to achieve the theoretical hydrogen gravimetric capacity of 7.4 wt %.

1 INTRODUCTION:

Hydrogen storage in complex hydrides has been extensively investigated as a safest and promising solution compared with the other technologies such as gas compression and liquefaction [1-2].

The wide interest towards the classes of light and complex hydrides, as borohydrides $\text{M}(\text{BH}_4)$ and alanates $\text{M}(\text{AlH}_4)$ is justified by their low molecular mass and high gravimetric storage capacities, up to 18 wt % H_2 in the case of LiBH_4 [3]. Unfortunately, due to the high thermodynamic stability, dissociation enthalpies of these compounds are near $200 \text{ kJ mol}^{-1} \text{ H}_2$, and working temperatures are too high for application purposes. To overcome it, multicomponent hydride systems based on the mixture of complex hydrides and light-metal hydrides represents an attractive class of materials [4, 5]. Similarly, systems with N-H bonds, as $\text{LiNH}_2 - \text{LiH}$, have high storage density (i.e. 9.6 wt %) but desorption occurs above 400°C [6]. The challenge is to develop synthetic strategies that allow modulating thermodynamic and kinetic properties in order to achieve an effective hydrides destabilization. The₂

thermodynamic performance of each hydride is controlled by the enthalpy and entropy of hydrogenation/dehydrogenation. The two quantities are correlated, and in the case of high enthalpy values, a considerable amount of energy is required to extract hydrogen, while the recharging process evolves important quantities of heat, hardly to be dispersed in a short time.

Optimal windows are estimated to lie in the 15 to 25 kJ mol⁻¹ and 90 to 110 J K⁻¹ mol⁻¹ ranges for dehydrogenation enthalpy and entropy, respectively [7]. Thus, the present focus of the hydrogen storage research is to produce a material, in pure or composite form, which can satisfy such values.

Thermodynamic calculations based on first-principles have represented a useful tool in order to find promising mixture of hydrides [8, 9]. In this contest, thanks to the implementation of crystal database (>200 solid compounds), Alapati and coauthors have explored a wide range of metal hydrides at different temperatures, detecting 43 very promising single-step reactions [10]. Most recently, D. S. Sholl et al, presented the largest set of thermodynamic calculations of reversible hydrogen storage systems using a database of 359 crystalline materials [11]. Among several systems identified, the LiNH₂-KBH₄-LiH mixture in the molar ratio 2:1:1 represents a very attractive composite: it shows a hydrogen gravimetric capacity of 7.48 wt. % and a theoretical ΔH_{300} value equal to 28.1 kJ/mol H₂ [11]. The van't Hoff plot based on the DFT calculations shows that for the one-step reaction $2\text{LiNH}_2 + \text{KBH}_4 + \text{LiH} \rightarrow \text{Li}_3\text{BN}_2 + \text{KH} + 4\text{H}_2$ the sorption temperatures are expected between 27 °C and 147 °C in a range of H₂ pressures from 1 to 100 bar, i.e. appropriate for reversible hydrogen storage applications [11]. These encouraging theoretical results suggest that this system is a good mixture for experimental study.

In this work, we investigated the thermal hydrogen desorption process of 2LiNH₂ + KBH₄ + LiH system, by using in-situ synchrotron radiation powder x-ray diffraction (SR-PXD), high-pressure differential scanning calorimetry (HP-DSC), and manometric measurements. The combination of these techniques gives a first tangible result of the reaction mechanism of the ternary system.

2 EXPERIMENTAL DETAILS

Commercial powders of KBH_4 (99% purity), LiNH_2 (95% purity) and LiH (95% purity) were purchased from Sigma-Aldrich. The ternary mixture of LiNH_2 - LiH - KBH_4 in a molar ratio 2:1:1 was prepared by manual mixing and subsequently grinded using a mortar inside a glove box device (MBraun- 20-G), with O_2 , N_2 and H_2O levels below 1 ppm. The phases involved during the desorption process were characterized by means of in-situ synchrotron powder x-ray diffraction (SR-PXD), performed at the beamline D3 in the research laboratory HASYLAB, DESY, Hamburg. For the experiment, a new high pressure sample cell designed for in situ monitoring of solid/gas reactions was utilized [12, 13]. The sapphire capillary was loaded with the as-prepared powders inside a glove box machine. The *in situ* measurement was performed at 1 bar of Ar pressure. Each XRPD pattern was collected with an exposure time of 60 s in the 2θ range of $2\text{--}40^\circ$, using a wavelength, λ , of 0.49902 \AA . The material was first heated from 30°C to 400°C with a heating rate of $5^\circ\text{C}/\text{min}$ and then kept for 15 min at 400°C . XRPD patterns were also collected during cooling step ($5^\circ\text{C}/\text{min}$). All the raw SR diffraction data were elaborated and converted to powder patterns by the use of the FIT2D program [14]. The different phases and their microstructural parameters were evaluated by fitting the XRD patterns using the MAUD (Materials Analysis Using Diffraction) Rietveld refinement software [15]. Manometric and calorimetric measurements were performed by a manometric apparatus (PCTPro-2000, Setaram & Hy-Energy) and a high-pressure calorimeter (Sensys DSC, Setaram, pressure measurement accuracy: 1% of reading), respectively. For the manometric apparatus, the experiments were carried out by heating about 300 mg of powder from room temperature to 400°C at $5^\circ\text{C}/\text{min}$ under static vacuum, followed by 150 min of isothermal step at 400°C . Regarding the calorimetric analysis (HP-DSC), the high-pressure cell of the calorimeter was loaded with 50 mg of the as-prepared sample in the glovebox under continuously purified atmosphere. The temperature programmed desorption (TPD) curves were obtained by heating the samples from room temperature up to 400°C with a scanning rate of $5^\circ\text{C}/\text{min}$ in an atmosphere of 1 bar of pure helium.

3 RESULTS AND DISCUSSION

The desorption analysis of the reacting $2\text{LiNH}_2\text{-KBH}_4\text{-LiH}$ mixture reveals a multistep path, displayed in Fig.1 as H_2 wt. % vs. time. The first desorption step starts at around $150\text{ }^\circ\text{C}$ with a release of about 1.0 wt. % of H_2 , while the second step takes places with much faster kinetics at $380\text{ }^\circ\text{C}$ resulting in a larger release of H_2 . The full dehydrogenation is reached after 20 min of thermal treatment at $400\text{ }^\circ\text{C}$ with a total weight loss of 7.40 wt % of H_2 , which is rather consistent with the theoretical gravimetric capacity of the system (7.48 wt. %).

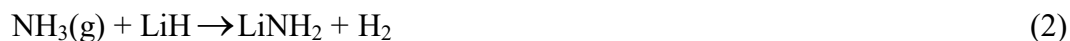
In order to define the sequences of reactions taking place during the desorption process, HP-DSC analysis was performed on the as-prepared hydride mixture.

The measurement, shown in Fig. 2, reveals three main peaks during the heating step: two exothermic peaks with onset at 160°C (A) and 330°C (B), respectively, and one strong endothermic peak at $360\text{ }^\circ\text{C}$ (C). Concerning the cooling step, three exothermic events at $260\text{ }^\circ\text{C}$ (D), $210\text{ }^\circ\text{C}$ (E) and $160\text{ }^\circ\text{C}$ (F), are detected. According to the manometric measurement reported in Fig. 1 a significant release of gas is only observed for the reactions that correspond to A and C peaks, confirming a multi-step desorption reaction.

To clarify exhaustively the desorption reaction mechanism, in-situ SR-PXD were performed on the $2\text{LiNH}_2\text{-KBH}_4\text{-LiH}$ mixture, applying the same thermal treatment conditions used in the HP-DSC analysis.

Fig. 3 shows the series of patterns collected from room temperature to $400\text{ }^\circ\text{C}$ with a scanning rate of $5^\circ\text{C}/\text{min}$. At room temperature the starting material reflections corresponding to the crystalline phases of KBH_4 and LiNH_2 are detected. LiH peaks are instead overlapped to those of KBH_4 . In addition, small traces of LiOH are also detected. The presence of LiOH is most likely due to a partial oxidation of as-

received LiH (see also Fig. 4 A). During heating, all peaks are shifted to lower 2θ angle because of the continuous increase in the lattice cell parameters of the phases associated with the thermal expansion. As also indicated by DSC (event A in Fig. 2), around 160°C a first transformation occurs (blue dash in Fig. 3), corresponding to the formation of Li_2NH from the reaction of LiNH_2 and LiH. To reinforce this, single XRPD scan (# 45) recorded at 166 °C is shown in Fig. 4 B. As reported in literature [16] the decomposition of LiNH_2 starts at 200 °C; however it was demonstrated that the addition of LiH in different molar ratio contributed to decrease the decomposition temperature [17]. Furthermore, this reaction is accompanied by the evolution of ammonia and hydrogen as shown in the following:



The global reaction is assumed to be [18]:



As displayed in Fig. 3, lithium imide and lithium amide are still present at temperatures over 350 °C (scan #110), and in particular the intensity associated with the LiNH_2 reflections significantly increase during this step, as also confirmed in Fig. 4 C. This aspect is probably ascribed to a coherent scattering domain growth of the LiNH_2 crystals before of the full decomposition. Around 380 °C, corresponding to the scan number 115 in Fig. 3, some yet unassigned peaks appear with a significant decrease of the LiNH_2 , Li_2NH and KBH_4 diffracted intensities. The unassigned phase is found to be stable just below 400 °C, and then its diffraction peaks disappear during the isothermal treatment.

The formation of the tetragonal Li_3BN_2 phase is observed at 400 °C (scan #120), while the LiNH_2 , Li_2NH and KBH_4 diffracted intensities are vanished. As also resulted from the scan 120, the KBH_4 disappearance is followed by the background increasing at low 2θ angle that can be associated to a molten phase. At the end of the annealing process, only Li_3BN_2 and molten phases are detected in the

patterns as evinced by Fig. 4. D. The formation of the Li_3BN_2 phase was also reported in a previous work by S. Orimo et al. [19]. They proved that the $\text{LiNH}_2/\text{LiBH}_4$ system in the molar ratio 2:1 desorbs hydrogen forming $\text{Li}_3\text{BN}_2\text{H}_8$, $\text{Li}_3\text{N-BN}$ and Li_3BN_2 . To the contrary, in this work the formation of $\text{Li}_3\text{BN}_2\text{H}_8$ is not observed in the in-situ XRD measurements. A possible explanation for the not observed phase is that, in the ternary system, KBH_4 starts to decompose only after 380 °C, whereas $\text{Li}_3\text{BN}_2\text{H}_8$ melts already at about 200 °C. Further experimental investigations are required to clarify the Li_3BN_2 formation from the reaction of Li_2NH , LiH and KBH_4 .

During the cooling step (not shown here), at roughly 260°C the formation of KH and the crystallization of potassium, the latter in a form stabilized at high pressure, with the vanishing of the diffuse halo are achieved. Both processes are linked to the exothermic peaks observed in the HP-DSC analysis during the cooling. As shown in Fig. 4 E, no further changes occur during cooling until the measurement was stopped at 25 °C. It is interesting to note that, in accordance with the theoretical study of D. S. Sholl et al [11], the formation of KH, as well as that of the ternary phase Li_3BN_2 , is experimentally demonstrated. However, one step desorption reaction is not observed and partial decomposition of KH is achieved at 400 °C. On this way, more efforts have to be devoted to decrease the hydrogen desorption temperature and understand the chemical nature of the unknown phase.

4 CONCLUSIONS

In this work we reported an experimental study on the decomposition of the $2\text{LiNH}_2 - \text{KBH}_4 - \text{LiH}$ system. It was observed that the desorption of the 2:1:1 mixture follows a multi-step reaction with a total weight loss of 7.40 wt % of H_2 , consistent with the theoretical gravimetric capacity of the system (7.48 wt. %). In-situ SR-PXD and HP-DSC experiments were performed to study the dehydrogenation mechanism and characterize the decomposition products. During heating, the partial decomposition of

LiNH_2 was accompanied by the formation of Li_2NH at 160°C with a small release of gas. At higher temperature, around 380°C , the reflections of the LiNH_2 , Li_2NH and KBH_4 phases completely disappeared to give a diffuse halo corresponding to a liquid-like phase plus an unstable unassigned phase. This step was characterized by a strong release of hydrogen. In addition, the ternary phase Li_3BN_2 was also detected. Upon cooling, the halo was vanished and, in addition to the Li_3BN_2 phase, there was weak appearance of KH and K cubic phases. Interesting, the formation of Li_3BN_2 and KH was also expected by theoretical calculations, but the experimental temperature at which the reaction occurred was considerably higher ($T_{\text{exp}} = 400^\circ\text{C}$ vs $T_{\text{th}} = 30^\circ\text{C}$). However, considering that no experimental evidences have been achieved up to now for this attractive system, the present results bring new contributes to the study of the reaction mechanism of the $2\text{LiNH}_2 + \text{LiH} + \text{KBH}_4$ mixture.

ACKNOWLEDGMENT: This work was funded by COST Action MP1103: “Nanostructured Materials for Solid State Hydrogen Storage”, by MIUR (Italian Ministry for University and Research), in the frame of the PRIN Project “Synthesis, characterization and functional evaluation of light hydrides-based nanostructured materials and nanoparticles for solid state hydrogen storage”, and by University of Sassari. S.G. acknowledges his postdoctoral fellowship, supported by the Fondazione Banco di Sardegna. Authors acknowledge beamline D3 in the research laboratory HASYLAB, DESY.

FIGURE CAPTIONS:

Figure 1.

Fig. 1. Thermal programmed desorption profile acquired on the $2\text{LiNH}_2 + \text{KBH}_4 + \text{LiH}$ mixture. Manometric signal: solid line. Temperature profile: dash-dotted line.

Figure 2.

Fig. 2. Calorimetric signal corresponding to the dehydrogenation process of the $2\text{LiNH}_2 - \text{KBH}_4 - \text{LiH}$ mixture). Calorimetric profile: solid line. Temperature profile: dashed line.

Figure 3.

Fig. 3. In-situ SR- PXD measurements of the $2\text{LiNH}_2 - \text{KBH}_4 - \text{LiH}$ mixture (2D plot). The analysis was carried out under 1 bar of Ar, heating the material from RT to 400°C ($5^\circ\text{C}/\text{min}$) and then keeping it for 15 min under isothermal conditions at 400°C . The thermal profile (red line) is reported as a function of the time and pattern scans.

Figure 4.

Fig. 4. In-situ SR- PXD patterns of the mixture collected at the temperature of 40°C (A), 166°C (B), 355°C (C), 400°C (D) during heating, followed by cooling at 300°C (E) and 40°C (F). Dots are experimental data, full red lines are from the Rietveld fit. The bars at the bottom indicate the line positions expected for each phase appearing in the various patterns examined.

REFERENCES:

- [1]. L. Schlapbach, A. Züttel, Hydrogen-storage materials for mobile applications, *Nature*. 414 (2001) 353-8.
- [2]. S. Orimo, Y. Nakamori, J.R. Eliseo, A. Züttel, CM Jensen, Complex Hydrides for Hydrogen Storage, *Chem Rev.* 107 (2007) 4111-4132.
- [3]. J. Graetz, New approaches to hydrogen storage, *J. Chem Soc Rev.* 38 (2009) 73-82.
- [4]. Garroni, S, Milanese, C, Girella A, Marini A, Mulas G, Menéndez E, Pistidda C, Dornheim M, Suriñach S, Baró MD. Sorption properties of $\text{NaBH}_4/\text{MH}_2$ (M=Mg, Ti) powder systems. *Int. J. Hydrogen Energy*. 2010; 35: 5434-41.
- [5]. Milanese C, Garroni S, Girella A, Mulas G, Berbenni V, Bruni G, Suriñach S, Baró MD, Marini A. Thermodynamic and kinetic investigations on pure and doped $\text{NaBH}_4\text{-MgH}_2$ system. *J. Phys. Chem. C*. 2011; 115: 3151-62.
- [6]. P. Chen , Z.T. Xiong, J.Z. Lou, J.Y. Lin, K.L. Tan, Interaction of hydrogen with metal nitrides and imides, *Nature*. 420 (2002) 302-304.
- [7]. WIF David, Effective hydrogen storage: a strategic chemistry challenge, *Faraday Discuss.* 151 (2011) 399-414.
- [8]. A. R. Akbarzadeh, V. Ozolins and C. Wolverton, First-Principles Determination of Multicomponent Hydride Phase Diagrams: Application to the Li-Mg-N-H System, *Adv. Mater.* 19 (2007) 3233–3239.
- [9]. V. Ozolins, E. H. Majzoub and C. Wolverton, First-Principles Prediction of Thermodynamically Reversible Hydrogen Storage Reactions in the Li-Mg-Ca-B-H System, *J. Am. Chem. Soc.*, 131 (2009) 230–237.
- [10]. S.V. Alapati, J.K. Johnson, D.S. Sholl, Large-Scale Screening of Metal Hydride Mixtures for

High-Capacity Hydrogen Storage from First-Principles Calculations, *J. Phys Chem C*. 112 (2008) 5258–5262.

- [11]. K. C. Kim, A. D. Kulkarni, J. K. Johnson, and D. S. Sholl, Large-scale screening of metal hydrides for hydrogen storage from first-principles calculations based on equilibrium reaction Thermodynamics, *Phys. Chem. Chem. Phys.* 13 (2011) 7218-7229.
- [12]. U. Bösenberg, S. Doppiu, L. Mosegaard, G. Barkhordarian, N. Eigen, A. Borgschulte, T.R. Jensen, Y. Cerenius, O. Gutfleisch, T. Klassen, M. Dornheim, R. Bormann, Hydrogen sorption properties of $\text{MgH}_2\text{--LiBH}_4$ composites, *Acta Mater.* 55 (2007) 3951-8.
- [13]. C. Pistidda, S. Garroni, C.B. Minella, F. Dolci, T.R. Jensen, P. Nolis, U. Bosenberg, Y Cerenius, W. Lohstroh, M. Fichtner, M.D. Baró, R. Bormann,R. Dornheim, Pressure Effect on the $2\text{NaH} + \text{MgB}_2$ Hydrogen Absorption Reaction, *J. Phys.Chem.C*. 114 (2010) 21816–21823.
- [14]. <http://www.esrf.eu/computing/scientific/FIT2D/>.
- [15]. P. Scardi, L. Lutterotti & P. Maistrelli, "Experimental Determination of the Instrumental Broadening in the Bragg-Brentano Geometry". *Powder Diffraction.*, 9 (1194), 180-186.
- [16]. P. Cheng, Z. Xiong, J. Luo, J. Lin, Interaction between Lithium Amide and Lithium, Hydride J. *Chem.*, B 107 (2003) 10967-10970.
- [17]. G. Miceli, C. S. Cucinotta, M. Bernasconi, M. Parrinello, First Principles Study of the $\text{LiNH}_2/\text{Li}_2\text{NH}$ Transformation, *J. Phiys. Chem.*, B114 (2010) 15174-15183.
- [18]. W.I.F. David, M. O. Jones, D. H. Gregory, C. M. Jewell, S. R. Johnson, A. Walton, P. P. Edwards, A mechanism for non-stoichiometry in the lithium amide/lithium imide hydrogen storage reaction, *J. Am. Chem. Soc.* 129 (2007) 1594-1601.
- [19]. Y. Nakamori, A. Ninomiya, G. Kitahara, M. Aoki, T. Noritake, K. Miwa, Y. Kojima, S. Orimo, Dehydriding reactions of mixed complex hydrides, *J. Power Sources* 155 (2006) 447-455.

